International Journal of Microwave and Wireless Technologies

cambridge.org/mrf

Compact ultra-wideband bandpass-response power divider with high-frequency selectivity

Song Guo, Kaijun Song, Yedi Zhou and Yong Fan

EHF Key Lab of Fundamental Science, School of Electronic Engineering, University of Electronic Science and Technology of China, Chengdu 611731, China

Research Paper

Cite this article: Guo S, Song K, Zhou Y, Fan Y (2018). Compact ultra-wideband bandpass-response power divider with high-frequency selectivity. *International Journal of Microwave and Wireless Technologies* **10**, 1107–1112. https://doi.org/10.1017/S1759078718001216

Received: 7 January 2018
Revised: 24 July 2018
Accepted: 26 July 2018
First published online: 13 September 2018

Key words:
Bandpass response; compact; high-frequency selectivity; power divider; ultra-wideband

Author for correspondence:
Song Guo, E-mail: 15528122037@163.com

Abstract

The ultra-wideband bandpass-response power divider with high-frequency selectivity is presented in this paper. This power divider consists of an impedance transformer, a filter network, and two isolation resistors. In order to realize the ultra-wideband filtering performance, parallel coupling lines and parallel open-circuit branches are applied to the second impedance converter. A resistor is added to the ends of the coupling lines to achieve good isolation and output return loss. The equivalent-circuit method is employed to analyze the presented power divider. The power divider, working at 3.45–8.29 GHz, is designed and fabricated. Two transmission zeros are generated at 2.8 and 9 GHz, respectively, and the out-of-band suppression is >13 dB. The measured results are in good agreement with the simulation ones.

Introduction

Recent advances in wireless communication systems have increased the demand for microwave passive [1–13] circuits with compact size to propose ultra-wideband [2, 5, 9, 14–17]. As one of the key devices, power divider is widely studied by scholars. More compact circuit size with wider bandwidth has become an important research direction. Wilkinson divider as the most widely used power divider has good isolation performance [18], but its bandwidth cannot meet the demand of ultra-wideband. In order to achieve ultra-wideband, some ultra-wideband power dividers have been developed [1, 2, 14, 16]. In [19], a design formula of multi-section power divider is derived to obtain wide isolation performance. However, this method requires a larger circuit size and more resistance, which are not conducive to integration. Recently, a few ultra-wideband power dividers [14, 20] based on the coupling structure were developed in order to achieve a high-frequency selectivity characteristics.

In this paper, a compact power divider is presented with ultra-wideband bandpass response. The nested structure makes the circuit more compact. Open-circuit microstrip lines are loaded at the ends of parallel-coupled lines to achieve ultra-wideband and high-frequency selectivity. Two resistors are designed to improve the isolation within the passband. Through the even–odd mode analysis, the relationship between the two isolation resistances is demonstrated. To verify the validity of the proposed design concept, an ultra-wideband power divider is fabricated and measured. Measured results agree well with the simulated ones.

Structure, analysis, and design

The layout of the proposed power divider is depicted in Fig. 1. The circuit structure can be divided into three parts: impedance converter, filter network, and isolation resistance. Impedance converters are designed in a nested form. The circuit structure is more compact than conventional multi-section impedance converters, achieving similar dimensions as single-node impedance converters. In order to achieve out-of-band rejection of the power divider, the distal impedance converter is replaced by a filter-type network. Parallel coupled lines and parallel open lines are designed to achieve ultra-wideband filtering performance. The end of the coupling line is connected by isolation resistor R_2, thus achieving good isolation and output return loss in the passband.

Since the circuit is symmetrical, the method of analyzing odd and even modes is applied to the design of the ultra-wideband bandpass-response power divider. Figure 2 shows the equivalent circuit model of the presented power divider, and the electrical length of each section satisfies the relationship: $\theta_1 = \theta_2/2$ and $(\theta_1 + \theta_2)/2 = \theta_A = \pi/2$. The equivalent circuit under

CAMBRIDGE UNIVERSITY PRESS

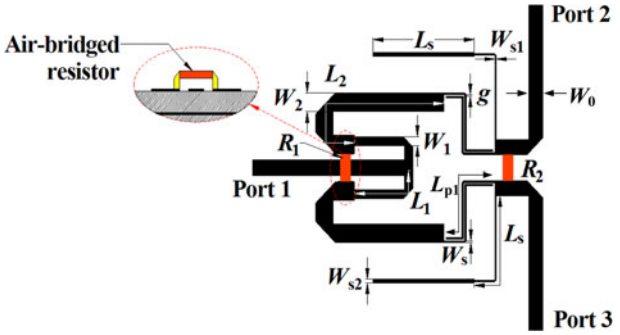

Fig. 1. Configuration of ultra-wideband power divider.

even-mode excitation is shown in Fig. 3(a), the transfer matrix of $[A]$ is :

$$[A] = [A]_{cl}[A]_{st} = \begin{bmatrix} a_2/Z_o+a_1 & a_2 \\ a_2/Z_o^2 + (a_1+a_4)/Z_o + a_3 & a_2/Z_o + a_4 \end{bmatrix}\begin{bmatrix} 1 & 0 \\ 1/Z_{st} & 1 \end{bmatrix} = \begin{bmatrix} a_2/Z_o + a_2/Z_{st} + a_1 & a_2 \\ a_2/Z_o^2 + a_2/Z_oZ_{st} + (a_1+a_4)/Z_o + a_4/Z_{st} + a_3 & a_2/Z_o + a_4 \end{bmatrix}, \tag{1}$$

where a_1, a_2, a_3, Z_o, Z_{st} can be expressed as:

$$a_1 = a_4 = (Z_{ce} + Z_{co})\cos\theta_A/(Z_{ce} - Z_{co}), \tag{2}$$

$$a_2 = -j/2[4Z_{ce}Z_{co}\cos^2\theta_A/(Z_{ce} - Z_{co})\sin\theta_A - (Z_{ce} - Z_{co})\sin\theta_A], \tag{3}$$

$$a_3 = j2\sin\theta_A/(Z_{ce} - Z_{co}), \tag{4}$$

$$Z_o = 2/(1/Z_{ce} + 1/Z_{co}), \tag{5}$$

$$Z_{st} = jZ_{s1}(Z_{s1}\tan\theta_{s1} - Z_{s2}\cot\theta_{s1})/(Z_{s1} + Z_{s2}). \tag{6}$$

The impedances seen from node T are further obtained as:

$$Z_{in}^{e1} = \frac{(a_2/Z_o + a_2/Z_{st} + a_1)Z_0 + a_2}{[a_2/Z_o^2 + a_2/Z_oZ_{st} + (a_1+a_4)/Z_o + a_4/Z_{st} + a_3]Z_0 + a_2/Z_o + a_4}, \tag{7}$$

$$Z_{in}^{e2} = Z_2\frac{Z_{in}^e + jZ_2\tan\theta_2}{Z_2 + jZ_{in}^e\tan\theta_2}, \tag{8}$$

where Z_{in}^e can be expressed as $Z_{in}^e = Z_1(2Z_0 + jZ_1\tan\theta_1)/(Z_1 + j2Z_0\tan\theta_1)$. In order to achieve good matching of the power divider under even-mode excitation, it must be satisfied $Z_{in}^{e1} = Z_{in}^{e2*}$. Therefore, the coupling between the odd–even mode impedance of the microstrip line and the impedance of the conversion line can be described by the following formula:

$$\frac{\frac{(Z_{ce}+Z_{co})Z_0}{Z_{ce}Z_{co}} + 2 + \frac{2Z_0}{Z_{st}}}{\frac{(Z_{ce}+Z_{co})^2Z_0}{2Z_{ce}^2Z_{co}^2} + \frac{8Z_0}{(Z_{ce}-Z_{co})^2} + \frac{(Z_{ce}+Z_{co})}{Z_{ce}Z_{co}} + \frac{Z_0(Z_{ce}+Z_{co})}{Z_{st}Z_{ce}Z_{co}}} = \left(\frac{Z_2(2Z_1Z_0 + j\sqrt{3}Z_1^2 + 6Z_2Z_0 - j\sqrt{3}Z_1Z_2)}{Z_2Z_1 + j2\sqrt{3}Z_2Z_0 - j2\sqrt{3}Z_1Z_0 + 3Z_1^2}\right)^*. \tag{9}$$

The condition $\mathrm{Re}(Z_{in}^{e1}) = \mathrm{Re}(Z_{in}^{e2*})$ can be obtained. When θ_{s1} is close to $\pi/2$ at center frequency, the relationship between Z_1, Z_2, Z_{ce}, and Z_{co} is simplified as

$$\frac{\frac{(Z_{ce}+Z_{co})Z_0}{Z_{ce}Z_{co}} + 2}{\frac{(Z_{ce}+Z_{co})^2Z_0}{2Z_{ce}^2Z_{co}^2} + \frac{8Z_0}{(Z_{ce}-Z_{co})^2} + \frac{(Z_{ce}+Z_{co})}{Z_{ce}Z_{co}}} \approx \frac{32Z_0Z_1^2Z_1^2}{(Z_1Z_2 + 3Z_1^2)^2 + 12Z_0(Z_1 - Z_2)^2}. \tag{10}$$

In the odd-mode excitation, the equivalent circuit model is shown in Fig. 3(b). From the impedance matching conditions $Z_{in}^{o1} = Z_{in}^{o2*}$, it can be deduced that:

$$\frac{\frac{(Z_{ce}+Z_{co})Z_0}{Z_{ce}Z_{co}} + \frac{4Z_0}{R_2} + 2 + \frac{2Z_0}{Z_{st}}}{\frac{(Z_{ce}+Z_{co})^2Z_0}{2Z_{ce}^2Z_{co}^2} + \frac{8Z_0}{(Z_{ce}-Z_{co})^2} + \frac{2(Z_{ce}+Z_{co})Z_0}{Z_{ce}Z_{co}R_2} + \frac{Z_{ce}+Z_{co}}{Z_{ce}Z_{co}} + \frac{Z_0(Z_{ce}+Z_{co})}{Z_{st}Z_{ce}Z_{co}}} = \left(\frac{Z_2(6Z_1Z_2 + j\sqrt{3}Z_1R_1 - j\sqrt{3}Z_2R_1)}{3Z_1R_1 + Z_2R_1 + j2\sqrt{3}Z_1Z_2}\right)^*. \tag{11}$$

The condition $\mathrm{Re}(Z_{in}^{o1}) = \mathrm{Re}(Z_{in}^{o2*})$ can be obtained. When θ_{s1} is close to $\pi/2$ at center frequency, the relationship between R_1 and R_2 is simplified as

$$\frac{\frac{(Z_{ce}+Z_{co})Z_0}{Z_{ce}Z_{co}} + \frac{4Z_0}{R_2} + 2}{\frac{(Z_{ce}+Z_{co})^2Z_0}{2Z_{ce}^2Z_{co}^2} + \frac{8Z_0}{(Z_{ce}-Z_{co})^2} + \frac{2(Z_{ce}+Z_{co})Z_0}{Z_{ce}Z_{co}R_2} + \frac{Z_{ce}+Z_{co}}{Z_{ce}Z_{co}}} \approx \frac{24Z_1^2Z_2^2R_1}{(3Z_1R_1 + Z_2R_1)^2 + 12(Z_1Z_2)^2}. \tag{12}$$

In order to achieve ultra-wideband filtering, a sufficiently large coupling coefficient is required. The coupling gap is given as $g = 0.1$ mm; $Z_{ce} = 171\ \Omega$ and$Z_{co} = 53\ \Omega$ are obtained by selecting and optimizing the appropriate coupling line width. Noted that according to (1) and multi-section ultra-wideband Wilkinson power divider circuit theory described in [19, 21], it is obtained from the calculation: $Z_1 = 69\ \Omega$, $Z_2 = 42\ \Omega$. According to (10), the relationship between R_1 and R_2 is given by:

$$\frac{3.27R_2 + 200}{0.07R_2 + 2.47} = \frac{2015.62R_1}{0.62R_1^2 + 1007.81}. \tag{13}$$

https://doi.org/10.1017/S1759078718001216 Published online by Cambridge University Press

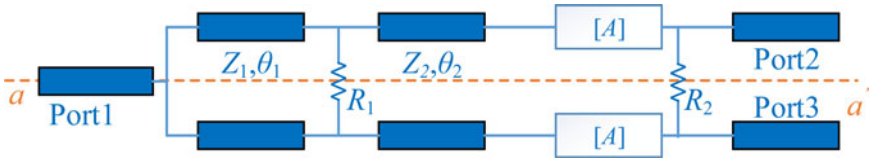

Fig. 2. Equivalent circuit for the proposed power divider.

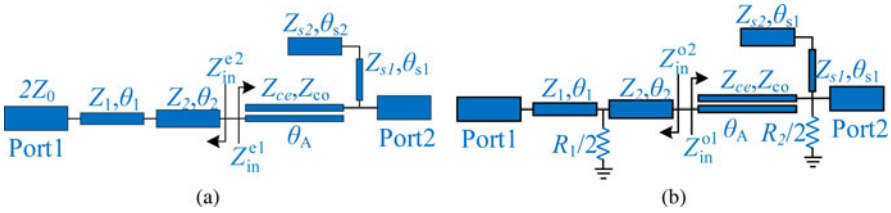

Fig. 3. (a) Even-mode equivalent circuit and (b) odd-mode equivalent circuit.

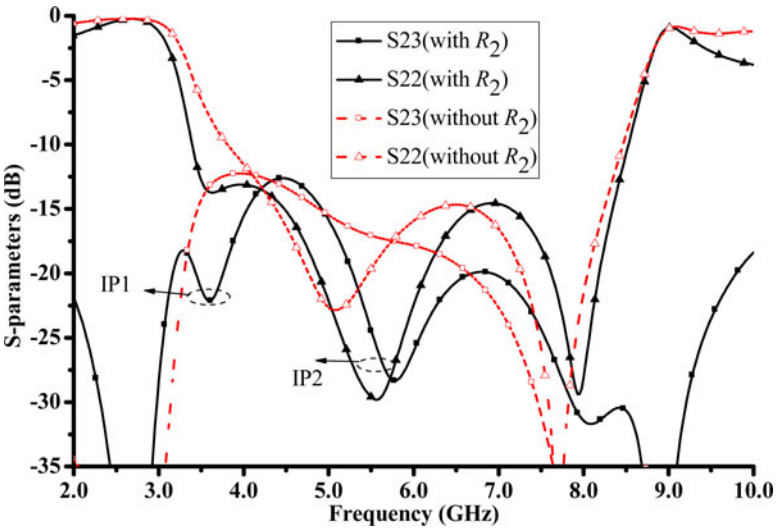

Fig. 4. Simulated output return loss and isolation for filters with and without R_2.

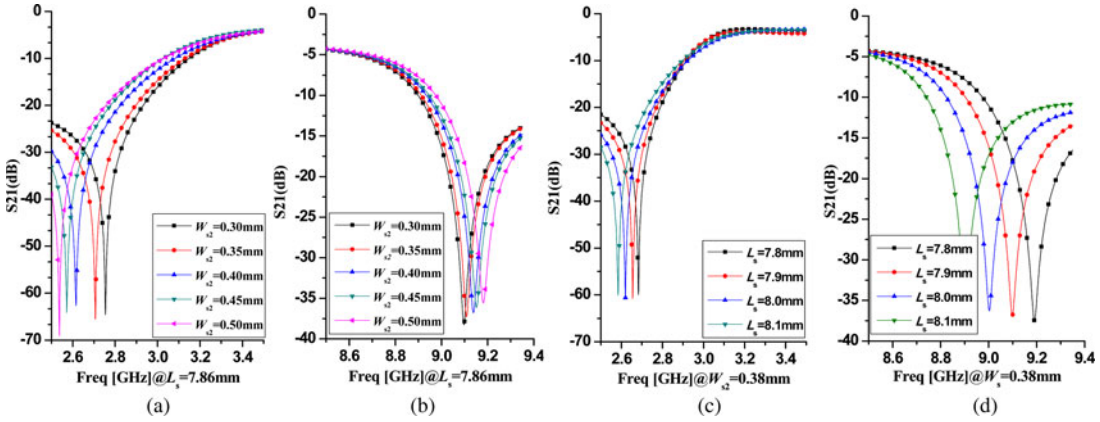

Fig. 5. The lower and upper TZ regions varied L_s and W_{s2}.

In Fig. 4, the effect of R_2 resistance on output return loss and isolation is demonstrated. When the isolation resistance is loaded at the end of the coupled microstrip line, the isolation curve produces two poles IP1 and IP2 at 3.58 and 5.77 GHz, respectively. At the same time, the output return loss is optimized at similar frequencies. R_2 effectively increases the isolation bandwidth and output return loss.

Based on the structure present in this paper, two transmission zeros (TZ) are generated at lower and upper regions, and the position is determined by the paralleled step impedance line

https://doi.org/10.1017/S1759078718001216 Published online by Cambridge University Press

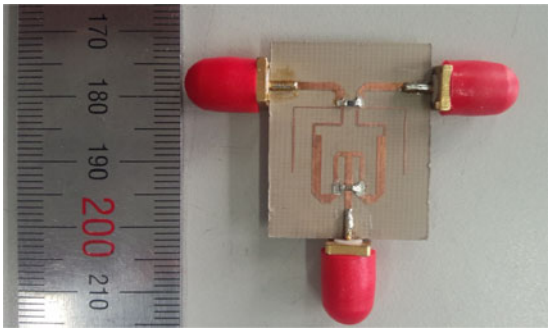

Fig. 6. Photograph of the power divider.

shown in Fig. 1. According to equation (6), when $Z_{s1}\tan\theta_{s1} = Z_{s2}\cot\theta_{s2}$ is satisfied, transmission zeros are generated at both ends. In order to simplify circuit parameters, always let $\theta_{s1} = \theta_{s2}$. So we can get:

$$\theta_0 = \theta_{s1} = \theta_{s2} = \arctan\sqrt{R_z}, \tag{14}$$

where $R_z = Z_{s1}/Z_{s2}$. The relationship between lower TZ frequency f_1 and upper TZ frequency f_2 can be expressed as

$$\frac{f_2}{f_1} = \frac{\theta_2}{\theta_1} = \frac{\pi - \theta_0}{\theta_0} = \frac{\pi}{\arctan\sqrt{R_z}} - 1. \tag{15}$$

According to equations (4)–(6), the position of the TZs at the lower and upper regions can be controlled by adjusting L_s, W_{s1}, and W_{s2} as shown in Fig. 1. Figure 5 shows the position of the lower TZ and the upper TZ with varied L_s and W_{s2}. It can be seen that the upper TZ shifts to the high end when the W_{s2} increases, while the lower TZ is opposite. When adjusting L_S, the two transmission zeros move in the same direction. According to such characteristics, the TZ's region can be adjusted appropriately.

Results and discussion

To verify the principle of the above design approach, an ultra-wideband bandpass power divider is designed and optimized by using full-wave simulation software HFSS 15.0. The layout is fabricated on the substrate Taconic RF-35 with a thickness of 0.508 mm and a loss tangent of 0.0018. In the simulation process, air bridge isolation resistance needs to be used, and the height of the solder at both ends is set to 0.6 mm. Through this modeling method, the simulation results are closer to the measured result. After simulation and optimization, the dimensions of the fabricated power divider are chosen as follows: $W_0 = 1.15$ mm, $L_1 = 5.93$ mm, $L_2 = 14.52$ mm, $L_S = 7.86$ mm, $W_1 = 0.66$ mm, $W_2 = 1.38$ mm, $W_{s1} = 0.12$ mm, $W_{s2} = 0.38$ mm, $W_s = 0.14$ mm, $g = 0.1$ mm, $L_p = 7.76$ mm, $R_1 = 82\ \Omega$, $R_2 = 240\ \Omega$. The real photograph of the ultra-wideband bandpass-response power divider is shown in Fig. 6. The final circuit size is 15.1 mm × 16 mm ($0.50\lambda_g \times 0.53\lambda_g$), which is the wavelength of the waveguide corresponding to the center frequency. Figure 7 shows the simulation and the measured results of the ultra-wideband bandpass-response power divider. As shown in Fig. 7(a), the designed power divider operates at 3.45–8.55 GHz with a relative bandwidth of 85%. The measured input return loss is better than 11 dB, and insertion loss

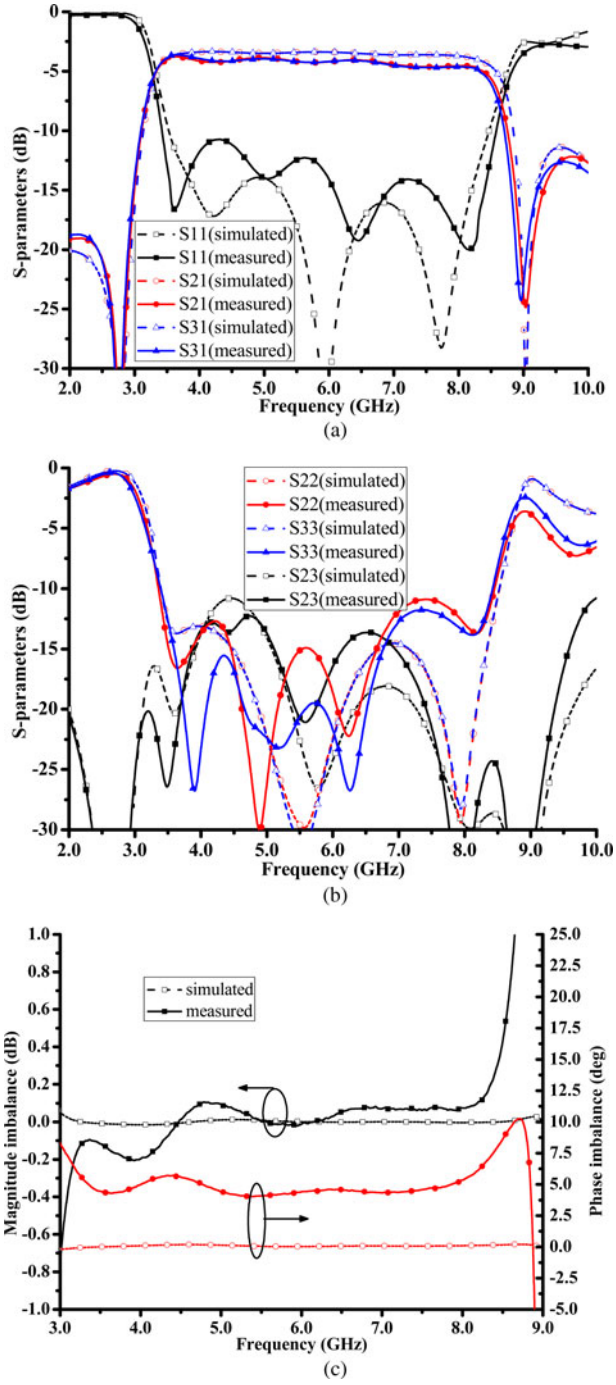

Fig. 7. Calculated, simulated, and measured frequency responses of the fabricated power divider: (a) insertion loss and input return loss, (b) output return loss, (c) magnitude imbalance and phase imbalance.

is better than 1.68 dB in the entire operating band range. Two transmission zeros are generated at 2.8 and 9 GHz and the out-of-band suppression is >13 dB. As shown in Fig. 7(b), output return loss is >13.2 dB in the band. The measured isolation between the output ports is >12.3 dB in the 2.45–8.29 GHz range. As shown in Fig. 7(c), the amplitude imbalance is within ±0.2 dB in the passband. The measured and the simulation results agree well with no frequency offset. The increase of insertion loss, especially in the high-frequency band, is mainly due to the increase of the distribution parameters of the isolation resistance

https://doi.org/10.1017/S1759078718001216 Published online by Cambridge University Press

Table 1. Comparisons between the proposed power divider and the reported ones

	Frequency (GHz)	10 dB (S_{11}) RBW (%)	Size ($\lambda g \times \lambda g$)	High selectivity
[19]	1–6	142	>0.5 × 1	No
[17]	3.5–9.8	94	0.33 × 0.37	No
[9]	1.27–2.8	75.2	0.52 × 0.69	Yes
This work	3.45–8.55	85	0.50 × 0.53	Yes

in the high-frequency band. Comparisons between the proposed and the previous ones are listed in Table 1. It can be found that the presented ultra-wideband power divider has the advantages of high-frequency selectivity. At the same time, assembly error of the SMA connector and substrate dielectric loss also increase insertion loss.

Conclusion

An ultra-wideband bandpass-response power divider is proposed and validated in this paper. The equivalent circuit of the presented power divider has been developed based on the even–odd mode analysis and has been used to design the presented power divider. The circuit is fabricated and measured. The measured results are in good agreement with the calculated and the simulation results. The power divider is easy to be fabricated and suitable for modern wireless systems.

Acknowledgement. This work was supported by the National Natural Science Foundation of China (Grant No: 61771094) and by the Research Fund of Shanghai Academy of Spaceflight Technology (Grant No: SAST2016094).

References

1. **Chiu L, Yum TY, Xue Q and Chan CH** (2006) A wideband compact parallel-strip 180 degrees Wilkinson power divider for push-pull circuitries. *IEEE Microwave and Wireless Components Letters* **16**, 49–51.
2. **Chiu L, Xue Q and Chan CH** (2008) A wideband compact parallel-strip 180 degrees Wilkinson power divider for push-pull circuitries. *Microwave and Optical Technology Letters* **50**, 3271–3274.
3. **Xue Q and Song K** (2010) Ultra-wideband coaxial-waveguide power divider with flat group delay response. *Electronics Letters* **46**, 1236-U98.
4. **Song K, Yuxia M, Quan X and Yong F** (2014) Wideband four-way out-of-phase slotline power dividers. *IEEE Transactions on Industrial Electronics* **61**, 3598–3606.
5. **Hu S, Kaijun S and Yong F** (2014) Ultra-wideband (UWB) eight-way ring-cavity power divider. *International Journal of Microwave and Wireless Technologies* **7**, 115–120.
6. **Tang C, Yong F and Kaijun S** (2015) A dual-band unequal power divider with flexible choice of implementation. *International Journal of Microwave and Wireless Technologies* **8**, 171–178.
7. **Song K, Abdullahi NA, Bingkun H, Yu Z, Fulong C and Yong F** (2015) Broadband six-way out-of-phase SIW power divider. *International Journal of Microwave and Wireless Technologies* **8**, 165–170.
8. **Song K, Liyuan X, Guoliang L, Maoyu F and Yong F** (2017) Novel four-way slotted-substrate integrated waveguide power divider using identical coupling circuits. *Electromagnetics* **37**, 233–239.
9. **Tang C, Xianqi L, Yong F and Kaijun S** (2015) A wideband power divider with bandpass response. *International Journal of Microwave and Wireless Technologies* **8**, 583–590.
10. **He Z, Kaijun S, Bo Z, Yu Z and Yong F** (2017) Miniaturized tri-band filtering-response power divider with short- and open-stub-loaded resonators. *International Journal of Microwave and Wireless Technologies* **9**, 1637–1643.
11. **Hu S, Kaijun S and Yong F** (2017) Compact multi-layer N-way power divider with closed-ring-shaped isolation network. *International Journal of Microwave and Wireless Technologies* **9**, 1945–1949.
12. **Song K, Te K, Xue R, Yu Z and Yong F** (2017) Miniaturized Bagley Polygon power divider by using composite right-/left-handed transmission lines. *International Journal of Microwave and Wireless Technologies* **9**, 1833–1837.
13. **Song K, Yifang Z, Maoyu F, Yu Z and Yong F** (2017) Wide-stopband bandpass-filtering power divider with high-frequency selectivity. *International Journal of Microwave and Wireless Technologies* **9**, 1931–1936.
14. **Wang X, Wang J and Zhang G** (2016) Design of wideband filtering power divider with high selectivity and good isolation. *Electronics Letters* **52**, 1389–1391.
15. **Ahmed UT and Abbosh AM** (2015) Modified Wilkinson power divider using coupled microstrip lines and shunt open-ended stubs. *Electronics Letters* **51**, 838–839.
16. **Zhuge CL, Song KJ and Fan Y** (2012) Ultra-wideband (UWB) power divider based on signal interference techniques. *Microwave and Optical Technology Letters* **54**, 1028–1030.
17. **Yang ZQ, Luo BY, Dong J and Yang T** (2016) Ultra-wideband power divider employing coupled line and short-ended stub. *Microwave and Optical Technology Letters* **58**, 713–715.
18. **Wilkinson EJ** (1960) An N-way hybrid power divider. *IRE Transactions on Microwave Theory and Techniques* **8**, 116–118.
19. **Sung-Won L, Kim C-S, Choi Kwan S, Park J-S and Ahn D** (2001) A general design formula of multi-section power divider based on singly terminated filter design theory. *2001 IEEE MTT-S International Microwave Symposium Digest (Cat. No.01CH37157), 20–24 May 2001*.
20. **Zhang B and Liu Y** (2015) Wideband filtering power divider with high selectivity. *Electronics Letters* **51**, 1950–1952.
21. **Song KJ, Hu BK, Duan Q, Chen QK and Fan Y** (2014) Ultra-wideband power divider with a notched band using embedded dual-mode resonators. *Microwave and Optical Technology Letters* **56**, 2758–2762.

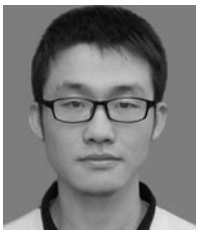

Song Guo was born in Lang Fang, Hebei Province, China, in February 1993. He received the B.Sc. degree in Microelectronics from Harbin Engineering University, Harbin, Heilongjiang, China, in 2006, and is currently working toward the M.Sc. degree in Electromagnetic Fields and Microwave Technology at the University of Electronic Science and Technology of China (UESTC). His research interests include microwave and millimeter-wave power-combining technology and microwave passive component design.

Kaijun Song (M'09-SM'12) received the M.S. degree in Radio Physics and the Ph.D. degree in Electromagnetic Field and Microwave Technology from the University of Electronic Science and Technology of China (UESTC), Chengdu, China, in 2005 and 2007, respectively. Since 2007, he has been with the EHF Key Laboratory of Science, School of Electronic Engineering, UESTC, where he is currently a Full Professor. From 2007 to 2008, he was a postdoctoral research fellow with the Montana Tech of the University of Montana, Butte, USA, working on microwave/millimeter-wave circuits and microwave remote-sensing technology. From 2008 to 2010, he was a research fellow with the State Key Laboratory of Millimetre Waves of China, Department of Electronic Engineering, City University of Hong Kong, on microwave/millimeter-wave power-combining technology and ultra-wideband (UWB) circuits. He was a senior visiting scholar with the State Key Laboratory of Millimetre Waves of

https://doi.org/10.1017/S1759078718001216 Published online by Cambridge University Press

China, Department of Electronic Engineering, City University of Hong Kong in November 2012. He has published more than 80 internationally refereed journal papers. His current research fields include microwave and millimeter-wave/THz power-combining technology; UWB circuits and technologies; microwave/millimeter-wave devices, circuits, and systems; and microwave remote-sensing technologies. Prof. Song is the Reviewer of tens of international journals, including *IEEE Transactions* and *IEEE Letters*.

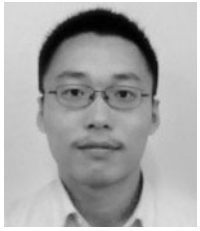

Yedi Zhou was born in Harbin, Heilongjiang Province, China, in January 1991. He received the B.S. degree from the University of Electronic Science and Technology of China (UESTC), Chengdu, China, in 2013. He is currently pursuing the Ph.D. degree in Electromagnetic Fields and Microwave Technology at UESTC. His research interests include microwave and millimeter-wave power-combining technology.

Yong Fan (M'05) received the B.E. degree from Nanjing University of Science and Technology, Nanjing, Jiangsu, China, in 1985 and the M.S. degree from the University of Electronic Science and Technology of China, Chengdu, Sichuan, China, in 1992. He is now with the School of Electronic Engineering, University of Electronic Science and Technology of China, where he is currently a Full Professor. His current research interests include electromagnetic theory, millimeter-wave technology, communication, and system. He has authored and co-authored over 130 papers. Mr. Fan is a senior member of the Chinese Institute of Electronics.

https://doi.org/10.1017/S1759078718001216 Published online by Cambridge University Press